https://erjm.journals.ekb.eg
ISSN: 1110-1180

DOI: ---------

ERJ
Engineering Research Journal
Faculty of Engineering
Menoufia University

Effect of Lateral Reinforcement Densification on the Axial Load Capacity of Reinforced Concrete Columns

Ibrahim G. Mahmoud [*], Magdy A. Tayel , and Mohamed A. Kandil

Department of Civil Engineering, Faculty of Engineering, Menoufia University, Egypt.

**(Corresponding author: ibrahimgalalmahmoud@gmail.com)*

ABSTRACT

The major reason for confining concrete columns is to avoid lateral expansion caused by the influence of Poisson's effect. The stirrups are used to resist the longitudinal bar's buckling and the effects of tensile stresses. This paper studies the effect of densification of stirrups in tied R.C. columns. To achieve this goal, two groups consisting of 14 specimens with different cross sections and different densifications of stirrups were tested under static axial loads. Group (A) consists of seven specimens with a cross section of 200x200 mm and a height of 1200 mm, and group (B) consists of seven specimens with a circular cross section with a diameter of 200 mm. The results indicated that increasing the ratio of stirrups' densification increases failure load and improves column behavior, also increasing the ratio of stirrups' densification enhances ductility. Stirrups' densification throughout the column's length is more effective than stirrups densification at the top and bottom. Increasing the percentage of stirrups' densification height at the top and bottom of the column leads to increasing the capacity of the column, and at the same time, it is more economical than increasing the dimensions of the column or increasing the main reinforcement.

Keywords: *Lateral reinforcement Densification; Axial load capacity; Experimental; Columns confinement.*

1. Introduction

The major reason for confining concrete columns is to avoid lateral expansion caused by the influence of Poisson's ratio. Because of the stress compatibility, concrete column confinement can improve column performance, such as capacity and deformability. Yet, rather than load-bearing capability, the effect of confinement is more obvious in enhancing ductility and post-peak-stress deformability. In general, transverse reinforcement in concrete columns serves two functions: keeping longitudinal reinforcement in place and confining concrete columns against lateral expansion. Numerous previous studies have attempted to clarify the influence of lateral reinforcement and densification on enhancing column performance, particularly in resisting vertical loads. Chang et al. [1] presented a paper that evaluates the strength and ductility of laterally confined concrete. To reach the purpose, the effects of the investigated parameters, including concrete strength, the volumetric ratio, tensile strength, configurations of transverse reinforcements, and the longitudinal reinforcement ratio, on the strength and ductility of laterally confined concrete were analyzed. The results showed that concrete strength, the volumetric ratio, configurations of transverse reinforcements, and the distribution of longitudinal reinforcements had an obvious influence on the strength and ductility of confined concrete.

Hou et al. [2] represented research about the effect of high-strength spirals on the behavior of high-strength concrete circular columns under axial compressive loads. It is concluded from the study that the higher the compressive strength of unconfined concrete, the lower the ratio of concrete tensile strength to compressive strength and poisson's ratio, and the more resistant the column is to shear sliding. Increasing the volumetric ratio resulted in both strength and strain increases.

Abd-Elhamed and Owida [3] Represented a study about the effect of lateral reinforcement densification in the top and bottom areas of the columns and along column lengths with different slenderness ratios (λ). It was observed that the failure load increases by increasing the densification of stirrups at the top and bottom of the column to the total column height.

Wasim et al. [4] examined three groups of columns. Each group consists of three columns. Based on the test results of this investigation, it was observed that the load-carrying capacity of a short, reinforced concrete column confined with a ferromesh jacket in addition to rings is 20% higher than the column confined using only 6 mm rings.

Liu et al. [5] examined 26 R.C. columns. The cross-sectional width of the tested columns ranged from 267 mm to 600 mm, and the height changed from 800 mm to 1800 mm. It is concluded from this study that the larger the stirrup ratio, the larger the triaxial confining pressure generated by stirrups, and the weaker the size effect the columns exhibit.

Du et al. [6] presented a paper dealing with an experimental investigation of stocky reinforced concrete (RC) columns confined by stirrups with a slenderness ratio of 3. The test observations indicate that increasing the stirrup ratio could enhance the nominal strength and improve the ductility capacity.

2. Aim and Research Significance

The current study is concerned with determining the influence of the following on the behavior of RC columns:

i. The effect of transverse reinforcement densification at the top and bottom zones, as well as along the length of columns, on the capacity of short reinforced concrete columns under static axial load.

ii. Determination of failure modes and physical changes for short columns with different ratios of stirrups' densification.

3. Experimental Program

Two groups consisting of 14 specimens, as illustrated in Table (1), were tested. Group (A) consists of R.C. short square columns with a cross section of 200 x 200 mm and a height of 1200 mm, as well as major reinforcing longitudinal steel of 4 Φ 12 mm bars and stirrups of Ø8 mm with a difference in densification along the height of the columns as shown in Figure (1). Group (B) consists of R.C. circular short columns with a diameter of 200 mm and a height of 1200 mm, with major reinforcing longitudinal steel of 6 Φ 10 mm bars and stirrups of Ø8 mm and a variation in densification along the columns' height as shown in Figure (2).

3.1 Materials

i. The coarse aggregate in the mix was crushed stone with a maximum nominal size of 16 mm.

ii. The fine aggregate in the mix was graded sand with sizes ranging from 0.075 to 4.75 mm.

iii. Ordinary Portland cement was utilized.

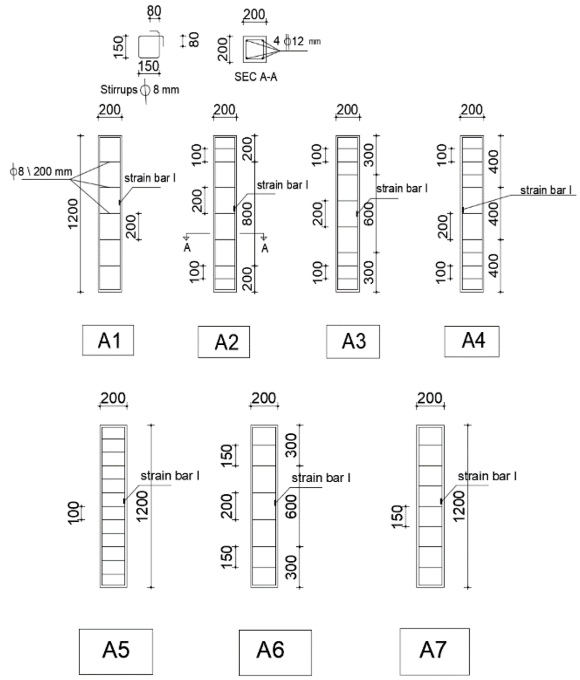

Figure 1–Details of specimens of group (A).

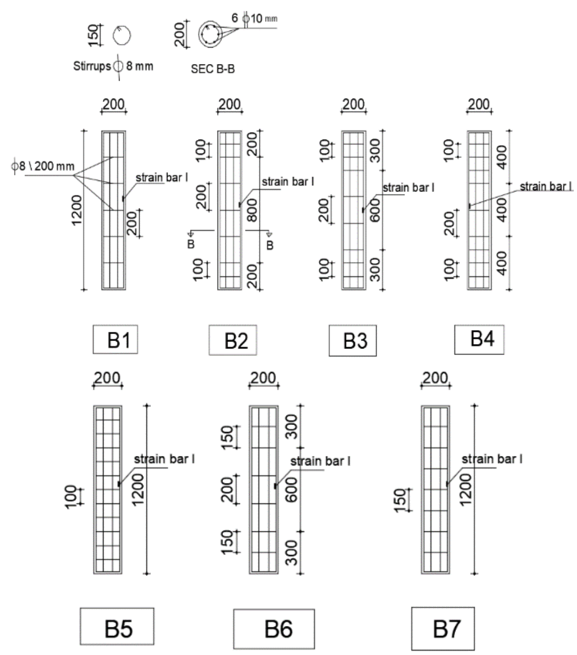

Figure 2–Details of specimens of group (B).

iv. For mixing and curing operations, ordinary tap water with no special taste, smell, color, or turbidity was utilized with water cement ratios of 45% and 50%.

v. The reinforcing steel utilized in this experiment is made locally. Including high-tensile steel bars with two diameters (Φ 10 and Φ 12 mm) with grade B500DWR and mild steel bars st24/37 with diameter (Ø 8 mm).

Table 1– Details of specimens

Group No.	Column No.	Column's dimension			Height of stirrups densification zones at top and bottom of columns (mm)	Total Stirrups Volumetric ratio [ρt.%]	% Of stirrups Densification height top and bottom / total column height	Long. steel ratio, [μ%]
		b (mm)	t (mm)	h (mm)				
A	A1	200	200	1200	0	0.44%	0%	1.13 %
	A2				400	0.565%	16.67%	
	A3				600	0.628%	25%	
	A4				800	0.691%	33.33%	
	A5				1200	0.817%	50%	
	A6				600	0.503%	25%	
	A7				1200	0.565%	50%	
B	B1	DIA. 200		1200	0	0.44%	0%	1.49 %
	B2				400	0.565%	16.67%	
	B3				600	0.628%	25%	
	B4				800	0.691%	33.33%	
	B5				1200	0.817%	50%	
	B6				600	0.503%	25%	
	B7				1200	0.565%	50%	

The specimens' concrete mixes were created in accordance with the Egyptian code of practice.

As illustrated in Table (2), the concrete mix was designed to achieve a target strength of 25 N/mm2 after 28 days. Table (3) illustrates the compressive strength for each group after testing sex cubes measuring 150x150x150 mm for each group.

3.2 Concrete dimensions and reinforcement details

Table (1) and Figures (1,2) illustrate the details of concrete dimensions and reinforcement for groups (A) and (B). Figures (3,4) illustrate steel cages for specimens.

3.3 Strain gauge and (LVDTs)

One electrical strain gauge was installed vertically at the midpoint of the main reinforcement of each specimen. Kyowa Measuring Instruments Co. Ltd., Tokyo, Japan, manufactured the strain gauges of the type KFGS- 10-120-C1-11L1 M2R, with a gauge length of 10 mm, gauge resistance of 120.4 $\Omega \pm 0.4$ %, gauge factor of 2.09 $\pm$ 1.0 %, transverse sensitivity ratio of 0.1 $\pm$ 0.2 %, and adoptable thermal expansion of $11.7 \times 10^{-6}/\ C^{0}$. Three LVDTs. were installed on columns to measure the lateral deformation. Figure (5) shows the location of the strain gauge and LVDTs.

3.4 Testing setup and procedure

All column specimens were examined under static axial loads at Tanta University's reinforced concrete laboratory. The loading frame was built to withstand the predicted maximum loads. Figures (6,7) illustrate the loading frame and test setup. As illustrated in Figure (6), the testing load was applied using a 2000 kN hydraulic jack. The data logger system shown in Figure (8) is connected to a load cell, LVDTs, and strain gauge and, at the same time, is connected to a computer with a software program to record the data.

4. Experimental Test Results

4.1 Failure modes

When the load increased, inclined cracks started to appear near the upper and lower parts of the column. After increasing the load, the cover spalled off, and it was observed that buckling started to occur in the longitudinal bars, and suddenly cutting in stirrups and crashing failure occurred. Figures (9,10) illustrate the failure modes of specimens.

4.2 Failure Loads

It was found that by increasing the ratio of stirrups' densification at the top and bottom as well as along the columns' height, the capacity of the columns increases. It was observed that increasing the ratio of

Table 2– Concrete mix design

Components	Mix ratios by weight for m^3 For Group (A)	Mix ratios by weight for m^3 For Group (B)
Coarse aggregate	12.94 kN	12.64 kN
Fine aggregate	6.47 kN	6.32 kN
Water	1.58 kN	1.75 kN
Cement	3.50 kN	3.50 kN
Water / cement ratio (w/c)	45%	50%

Table 3– Compressive strength for specimens after 28 days from casting.

Group	Compressive strength in N/mm^2
A	28
B	25

Figure 3 – Steel cages for group (A).

Figure 4 – Steel cages for group (B).

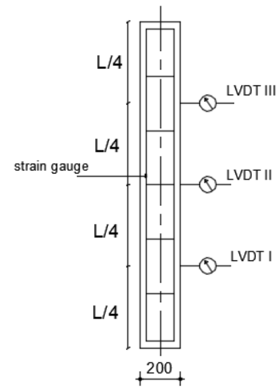

Figure 5 – Location of strain gauge and LVDTs.

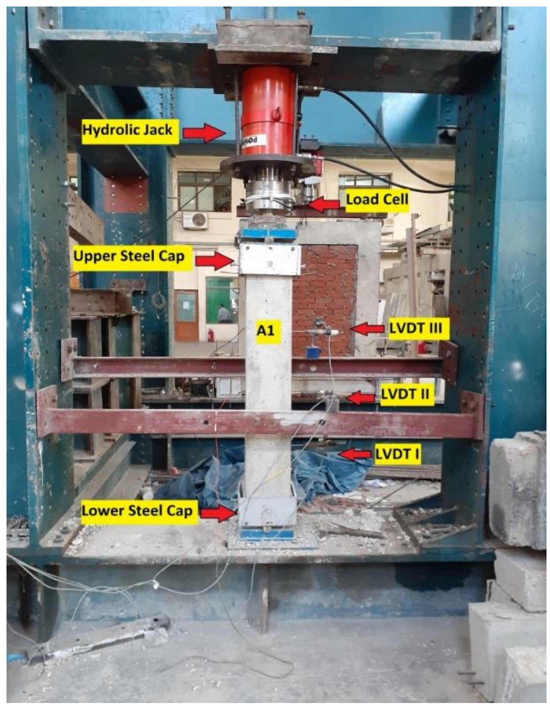

Figure 6 – The loading frame and test set up for group (A).

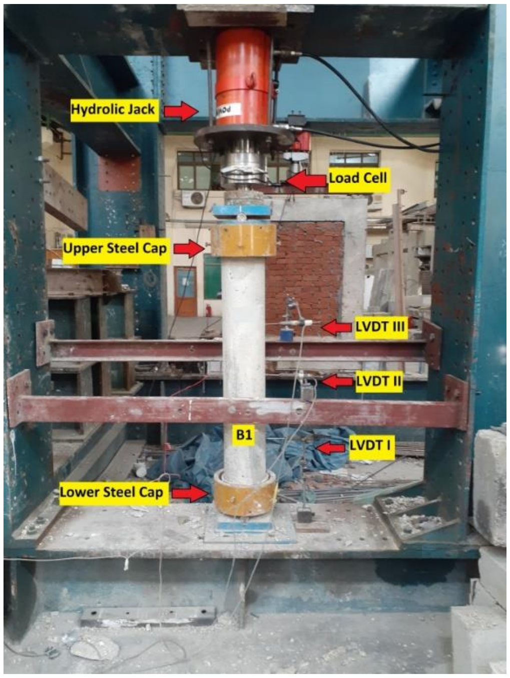

Figure. 7 – The loading frame and test set up for group (B).

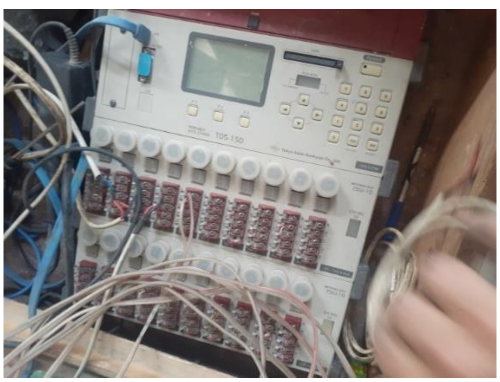

Figure 8– A 50 channel data logger (TDS -150) used in recording tests' results.

stirrups' densification led to improvements in the ductility of columns. For group (A), the control specimen A1 collapsed at a load of 1173 kN, while specimen A2 with a densification of 16.67% of height failed at a load of 1205 kN, with about a 3.00% increase in the column's strength. The specimen A3 with a densification of 25% of height and distance between stirrups at the densification zone equal to 100 mm failed at a load of 1275 kN, with about a 9.00% increase in the column's strength. The specimen A4 with a densification of 33.3% of height and distance between stirrups at the densification zone equal to 100 mm failed at a load of 1389 kN, with about an 18.00% increase in the column's strength. The specimen A5 with a densification of 50% of height and distance between stirrups at the densification zone equal to 100 mm failed at a load of 1560 kN, with about a 33.00% increase in the column's strength. The specimen A6 with a densification of 25% of height and distance between stirrups at the densification zone equal to 150 mm failed at a load of 1255 kN, with about a 7.00% increase in the column's strength. Finally, the specimen A7 with a densification of 50% of height and distance between stirrups at the densification zone equal to 150 mm failed at a load of 1525 kN, with about a 30.00% increase in the column's strength.

For group (B), the control specimen B1 collapsed at a load of 934 kN, while specimen B2 with a densification of 16.67% of height failed at a load of 983 kN, with about a 5.00% increase in the column's strength. The specimen B3 with a densification of 25% of height and distance between stirrups at the densification zone equal to 100 mm failed at a load of 1045 kN, with about a 12.00% increase in the column's strength. The specimen B4 with a densification of 33.3% of height and distance between stirrups at the densification zone equal to 100 mm failed at a load of 1140 kN, with about a 22.00% increase in the column's strength. The specimen B5 with a densification of 50% of height and distance between stirrups at the densification zone equal to 100 mm failed at a load of 1250 kN, with about a 34.00% increase in the column's strength. The specimen B6 with a densification of 25% of height and distance between stirrups at the densification zone equal to 150 mm failed at a load of 1020 kN, with about a 9.00% increase in the column's strength. Finally, the specimen B7 with a densification of 50% of height and distance between stirrups at the densification zone equal to 150 mm failed at a load of 1190 kN, with about a 27.00% increase in the column's strength.

Figure 9– Failure modes of group (A) from experimental results.

Figure 10– Failure modes of group (B) from experimental results.

Figures (11,12) illustrate comparisons between load-strain curves for specimens in each group.
Table (4) illustrates the ratio of densification of stirrups and the failure load of each column.

4.3 Increasing in Capacity

Figures (13,14) show the failure load and the percentage of increase in capacity for each specimen compared with the control specimen (the first specimen for each group).

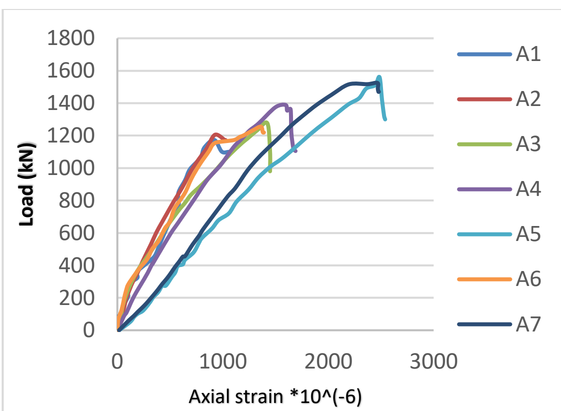

Figure 11– Vertical load-axial strain curve for all specimens of group (A) from experimental results.

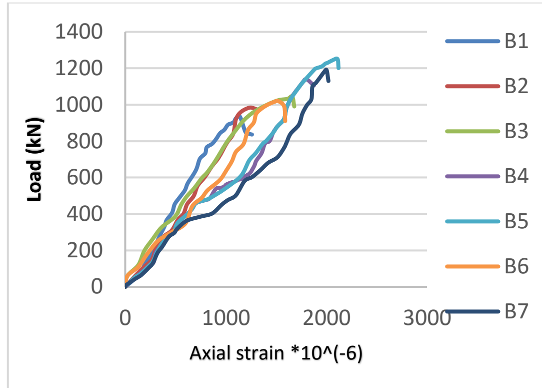

Figure 12– Vertical load-axial strain curve for all specimens of group (B) from experimental results.

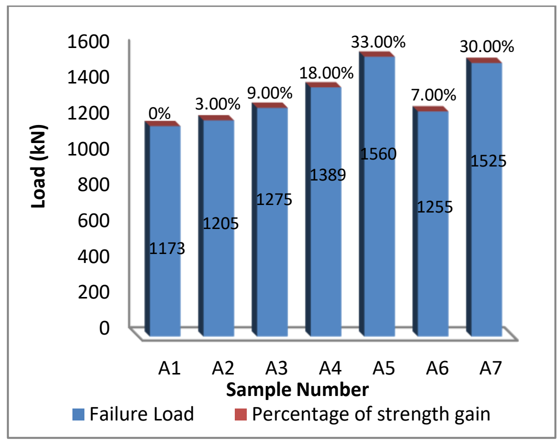

Figure 13– Failure loads and percentage of strength gained for tested specimens of group (A) from experimental results.

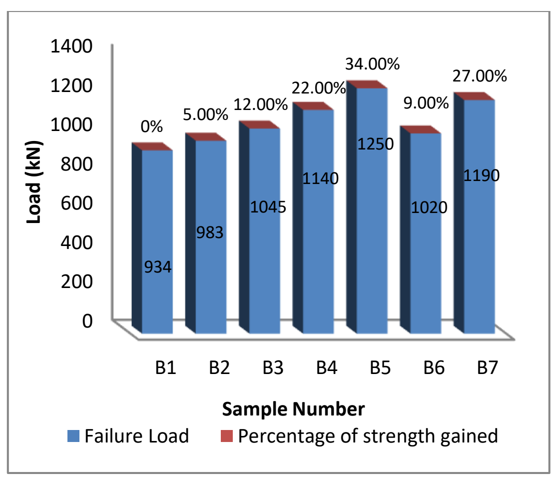

Figure 14– Failure loads and percentage of strength gained for tested specimens of group (B) from experimental results.

Table 4– Failure load of each specimen from experimental results.

Group No.	Column No.	% Of stirrups densification height top and bottom / total column height	Columns Dimension			Diameter of stirrups(mm)	Distance between stirrups in densification's zone (mm)	Long. steel ratio, [μ%]	Failure load (kN)
			b (mm)	t (mm)	h (mm)				EXP.
A	A1	0%	200	200	1200	8	0	1.13%	1173
	A2	16.67%					100		1205
	A3	25%					100		1275
	A4	33.33%					100		1389
	A5	50%					100		1560
	A6	25%					150		1255
	A7	50%					150		1525
B	B1	0%	Dia. 200 mm		1200	8	0	1.49%	934
	B2	16.67%					100		983
	B3	25%					100		1045
	B4	33.33%					100		1140
	B5	50%					100		1250
	B6	25%					150		1020
	B7	50%					150		1190

5. Theoretical Analysis

In this study, the F.E. program "ABAQUS 6.14-2" was adopted. The program takes into consideration the static or dynamic response and failure analysis of reinforced concrete structures in 2D, axisymmetric, or 3D space. In its analysis, the software employs a totally non-linear approach. The study uses a nonlinear iterative secant stiffness formulation and completely nonlinear material constitutive models for the reinforcement, concrete, and plates. The program divides the overall load exerted on the structure into user-defined phases for each analysis. The program iterates until the predefined convergence criterion is met to achieve convergence within each load step.

5.1 Finite Element Modeling

To create the finite element model, a 3D FE mesh of concrete panels and reinforcing bars is produced using two main types of components: solid element (C3D8R) for concrete and wire (beam) element (B31) for steel bars. The part option in the Abaqus model tree is used to define all element types utilized in the design of the finite element model.

5.2 Concrete Characteristics and Parameters

Concrete elastic characteristics and concrete damaged plasticity model parameters are listed in Tables (5,6). The modulus of elasticity of concrete was calculated according to the following relationship:

$E_c = 4400\sqrt{\sigma_{cu}}$ N/mm^2

Where σ_{cu} is the compressive strength after 28 days from casting.

Table 5– Elastic properties of concrete.

parameter	value
Density (t/m^3)	2.4
Poisson's Ratio (υ)	0.2

Table 6– Concrete damaged plasticity parameters.

parameter	value
Dilation Angle	35
Eccentricity	0.1
fb_0/fc_0	1.16
k	0.667
Viscosity parameter	0.00001

5.3 Elastic-plastic model for reinforcing bars

Steel represents an almost linear elastic behavior when the steel stiffness given by Young's modulus remains constant at low strain magnitudes. At higher strain magnitudes, it begins to produce nonlinear, inelastic behavior, which is referred to as plasticity. Steel's plastic nature is characterized by its yield point and post-yield hardening. The shift from elastic to plastic behavior on a material's stress-strain curve occurs at a yield point. Only elastic stresses are generated when steel is deformed before it reaches the yield point, and they are completely recovered when the applied force is released. However, when the stress in the steel reaches the yield stress, permanent (plastic) deformation occurs. Elastic and plastic stresses increase when the steel deforms in the post-yielding zone. The steel's stiffness decreases as the material yields. As a result of the plastic deformation, the yield stress of the steel material rises. The elastic properties of steel bars used in modelling are given in Table (7).

Table 7– The elastic properties of steel bars.

parameter	B240D-P	B500DWR
Density (t/m^3)	7.85	7.85
Poisson's Ratio (υ)	0.3	0.3
Modulus of Elasticity (Mpa)	200000	200000
Yield stress (Mpa)	240	500

5.4 Boundary Conditions

The following boundary conditions were chosen to represent the experimental conditions:

1. All nodes at the bottom of the column had transition constraints in the X, Y, and Z directions and rotation constraints about Y.

2. The perimeter nodes at the top of the column were restricted in the Z direction and in rotation about Y.

3. All other nodes had complete freedom to translate or rotate in any direction.

5.5 Contact Definition

In general, the contact surfaces of the concrete sample can be defined using "the interaction, create interaction property, and create interaction option" in relation to the interaction between the loads, reinforced mesh, and concrete sample. By defining contact surfaces, we describe all regions of the model that may come into contact with one another.

5.6 Creating Job in ABAQUS

We utilize the "create job" option to enable direct integration of a dynamic stress/displacement response in ABAQUS explicit analysis. To verify it, we must define the time of step in the ABAQUS software.

6. Results of Theoretical Investigation

6.1 Failure modes

Figures (15,16) illustrate the failure modes and stresses in steel bars of control specimens for group A and B.

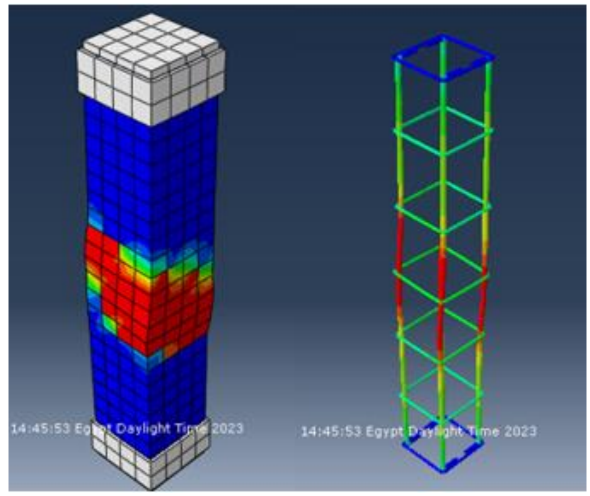

Figure 15– Failure mode and stresses in steel of specimen (A1) from theoretical results.

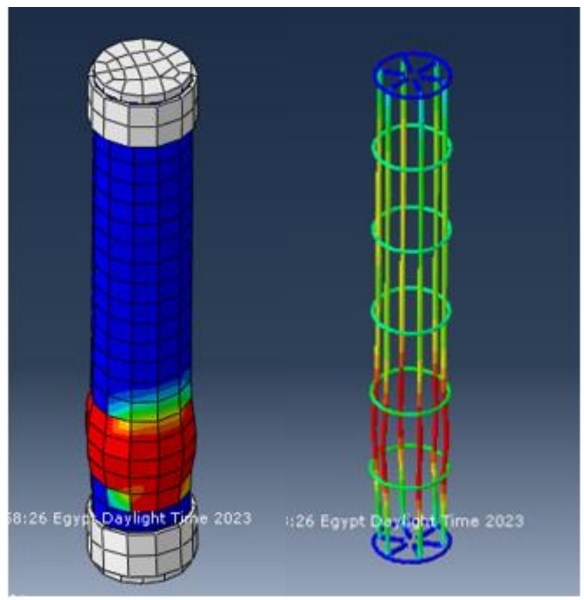

Figure 16– Failure mode and stresses in steel of specimen (B1) from theoretical results.

6.2 Failure Loads

It was observed that increasing the ratio of stirrups' densification led to an enhancement in the capacity and ductility of columns. Figures (17,18) illustrate comparisons between load-strain curves for specimens for each group. Table (8) illustrates the ratio of densification of stirrups and the failure load of each specimen.

Table 8– Failure load of each specimen from theoretical results.

Group No.	Column No.	% stirrups densification height top and bottom / total column height	Columns Dimension			Diameter of stirrups(mm)	Distance between stirrups in densification's zone (mm)	Long. steel ratio, [μ%]	Failure load (kN)
			b (mm)	t (mm)	h (mm)				Theoretical
A	A1	0%	200	200	1200	8	0	1.13%	1185
	A2	16.67%					100		1218
	A3	25%					100		1295
	A4	33.33%					100		1400
	A5	50%					100		1565
	A6	25%					150		1260
	A7	50%					150		1490
B	B1	0%	Dia. 200 mm		1200	8	0	1.49%	953
	B2	16.67%					100		1010
	B3	25%					100		1090
	B4	33.33%					100		1180
	B5	50%					100		1270
	B6	25%					150		1045
	B7	50%					150		1195

6.3 Increasing in Capacity

Figures (19,20) illustrate the failure load and the percentage of increase in capacity for each specimen compared with the control specimen (the first specimen for each group).

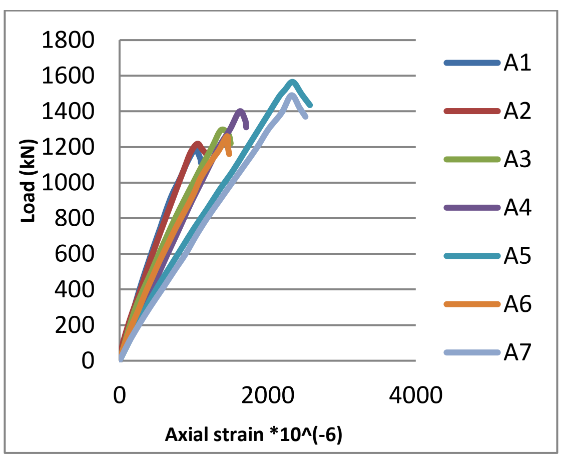

Figure 17– Vertical load-axial strain curve for all specimens of group (A) from theoretical results.

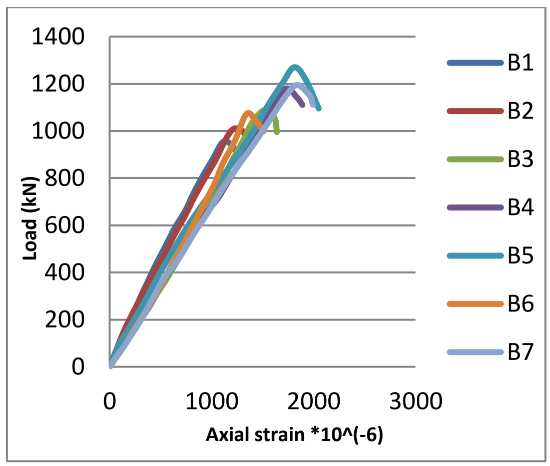

Figure 18– Vertical load-axial strain curve for all specimens of group (B) from theoretical results.

7. Comparison Between Experimental and Theoretical Results

A comparison study was conducted between experimental program results received by testing R.C. column samples and numerical results obtained from computer program execution. Table (9) shows the failure loads from both theoretical and experimental results. A maximum difference in failure load of 4.2% was observed between experimental and theoretical results.

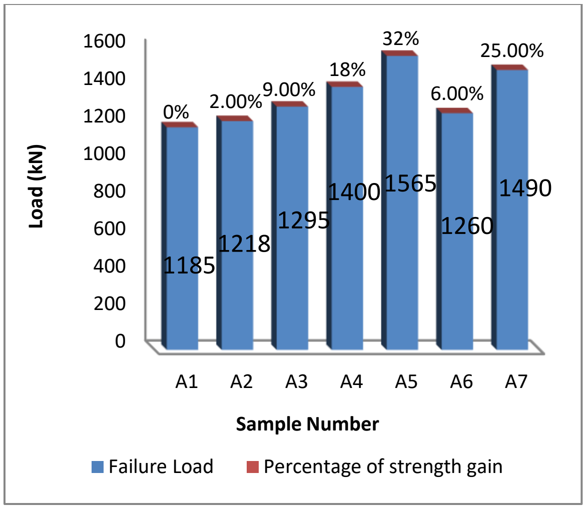

Figure 19– Failure loads and percentage of strength gained for tested specimens of group (A) from theoretical results.

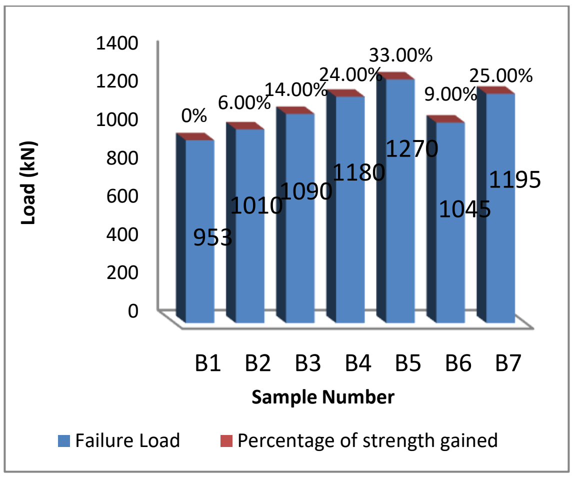

Figure 20– Failure loads and percentage of strength gained for tested specimens of group (B) from theoretical results.

Figures (21,22) show the percentage of increase in capacity for specimens and the difference between analytical and experimental results. A small difference in the percentage of increase in capacity of specimens was obtained from both theoretical and experimental results.

From failure modes obtained from experimental and theoretical analysis, it is observed that there are some differences in failure modes between experimental and theoretical results. First, in experimental analysis, there were many factors that affected the behavior of concrete, like compacting, curing, and the distribution of coarse and fine aggregate. These factors made the behavior of concrete different across the whole specimen, contrary to the theoretical analysis. Second, steel caps in the upper and lower of the specimens in the experimental work made some fixation to the sample, and stresses concentration happened in the upper and lower of the specimens. So, some specimens' failures happened near the end. Third, in theoretical analysis, the applied load is a totally axial load, but in experimental work, the applied load may not be a totally axial load. Perhaps some rotations or displacements occurred and caused these differences. Figure (23) shows the densification ratio versus the increase in capacity of tied R.C. short columns from the experimental and theoretical studies.

Table 9– Difference between failure loads from experimental and theorical results.

Sample	Load Failure (kN)		% of failure load from EXP. Results to FEM. analysis
	EXP.	FEM.	
A1	1173	1185	0.989
A2	1205	1218	0.989
A3	1275	1295	0.984
A4	1389	1400	0.992
A5	1560	1565	0.996
A6	1255	1260	0.996
A7	1525	1490	1.023
B1	934	953	0.98
B2	983	1010	0.973
B3	1045	1090	0.958
B4	1140	1180	0.966
B5	1250	1270	0.984
B6	1020	1045	0.976
B7	1190	1195	0.995

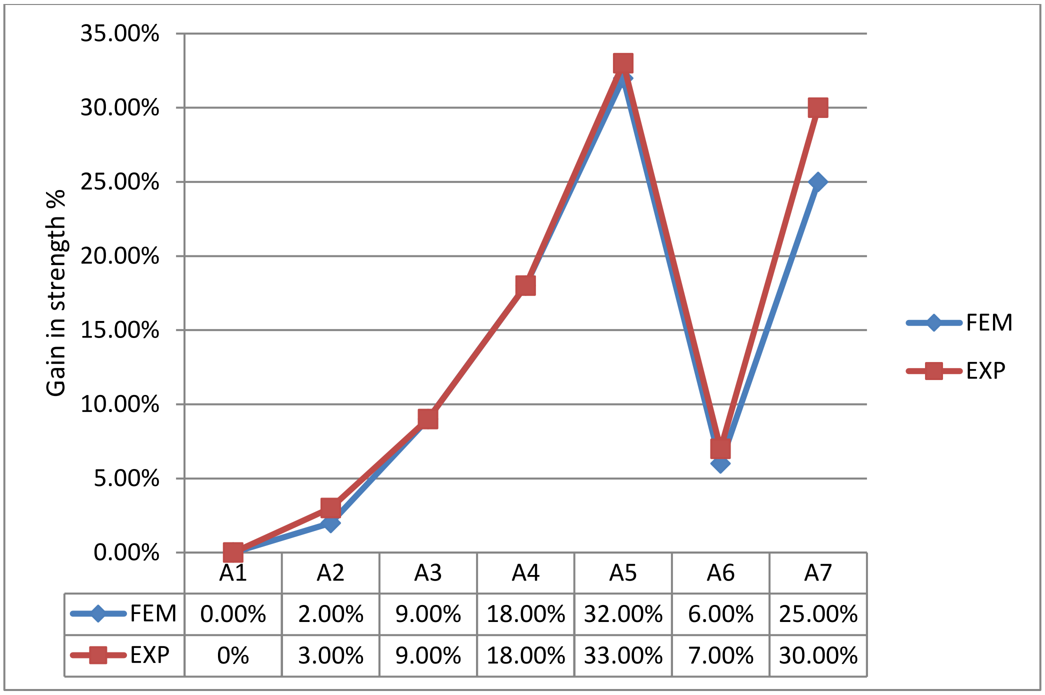

	A1	A2	A3	A4	A5	A6	A7
FEM	0.00%	2.00%	9.00%	18.00%	32.00%	6.00%	25.00%
EXP	0%	3.00%	9.00%	18.00%	33.00%	7.00%	30.00%

Figure 21–Comparison of strength gained percentage for specimens in group (A).

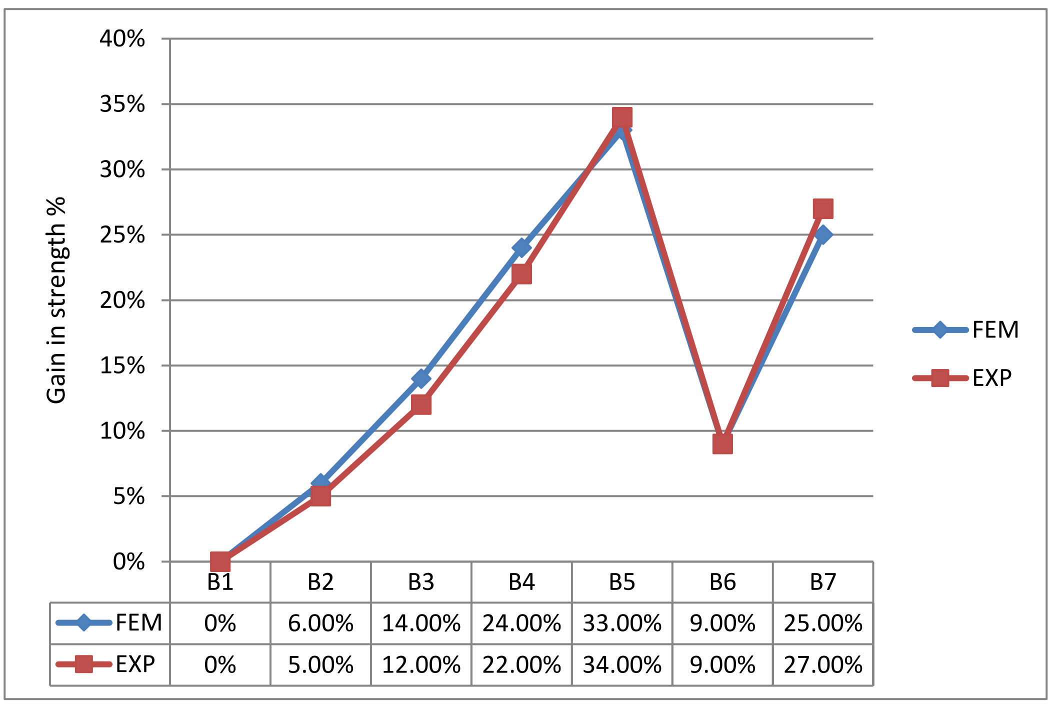

	B1	B2	B3	B4	B5	B6	B7
FEM	0%	6.00%	14.00%	24.00%	33.00%	9.00%	25.00%
EXP	0%	5.00%	12.00%	22.00%	34.00%	9.00%	27.00%

Figure 22–Comparison of strength gained percentage for specimens in group (B).

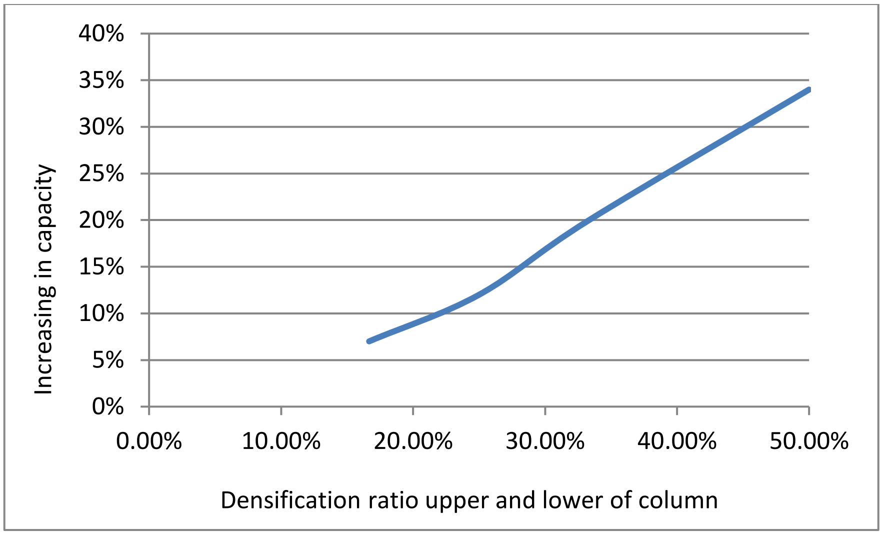

Figure 23– The concluded relationship between the densification ratio of stirrups in tied R.C. columns and the increase in capacity of columns.

8. Conclusions

From the present study, the following conclusions are obtained:

i. By increasing the percentage of stirrups' densification height at the top and bottom of the column to the total column height, the capacity of the column increases.

ii. Stirrups' densification throughout the column's length is more effective than stirrups densification at the top and bottom.

iii. By increasing the percentage of stirrups' densification height at the top and bottom of the column to the total column height, the ductility increases.

iv. Increasing the percentage of stirrups' densification height at the top and bottom of the column leads to increasing the capacity of the column, and at the same time, it is more economical than increasing the dimension of the column or increasing the main reinforcement.

v. The best performance of stirrups' configuration distance in the densification zone is not more than half the distance between the stirrups outside of the densification zone.

vi. Finite element models can determine the structural behavior of tested columns and are a better alternative to damaging laboratory tests.

9. References

[1] Chang, W., Hao, M., & Zheng, W., 2021. Strength and ductility of laterally confined concrete. Structural Concrete, 22(5), 2967-2991.

[2] Hou, C., Zheng, W. and Chang, W., 2020. Behaviour of high-strength concrete circular columns confined by high-strength spirals under concentric compression. Journal of Civil Engineering and Management, 26(6), pp.564-578.

[3] Abd-Elhamed, M.K. and Owida, M.E., 2019, August. Effect of stirrups densification on ultimate capacity of rectangular reinforced concrete columns. In Structures (Vol. 20, pp. 728-764). Elsevier.

[4] Razvi, S.W.N. and Shaikh, M.G., 2018. Effect of confinement on behavior of short concrete column. Procedia Manufacturing, 20, pp.563-570.

[5] Jin, L., Du, M., Li, D., Du, X. and Xu, H., 2017. Effects of cross section size and transverse rebar on the behavior of short squared RC columns under axial compression. Engineering Structures, 142, pp.223-239.

[6] Du, M., Jin, L., Du, X. and Li, D., 2017. Size effect tests of stocky reinforced concrete columns confined by stirrups. Structural Concrete, 18(3), pp.454-465.